JOURNAL OF GEOPHYSICAL RESEARCH, VOL. 104, NO. D16, PAGES 19,661–19,673, AUGUST 27, 1999

River basin hydrology in a global off-line land-surface model

Michael G. Bosilovich

Universities Space Research Association, NASA Data Assimilation Office, Greenbelt, Maryland

Runhua Yang[1]

General Sciences Corporation, NASA Data Assimilation Office, Greenbelt, Maryland

Paul R. Houser

NASA Hydrologic Sciences Branch and Data Assimilation Office, Greenbelt, Maryland

Abstract. Land-surface hydrology has been examined for the Off-line Land-surface GEOS Assimilation (OLGA) system and Goddard Earth Observing System (GEOS-1) data assimilation system using a river routing model. The GEOS-1 land-surface parameterization is very simple, using an energy balance prediction of surface temperature and prescribed soil water. OLGA uses atmospheric data from GEOS-1 to drive a more comprehensive parameterization of the land-surface processes. Using a global river routing model, OLGA's hydrology is evaluated against GEOS-1 (which serves as a control case) and observations. The river routing model moves monthly mean climatologic source runoff through river networks to simulate the river discharge from many river basins around the world, which can be compared to observed climatologic river discharge. Because of the soil hydrology, the OLGA system shows a general improvement in the simulation of river discharge, compared to the GEOS-1, by slowing the discharge of water. Snowmelt processes included in OLGA also have a positive effect on the annual cycle of river discharge and source runoff. The timing of the snowmelt in river discharge, however, still needs improvement in the annual cycle. Preliminary tests of a coupled land-atmosphere model indicate improvements to the hydrologic cycle compared to the uncoupled system. The river routing model has provided a useful tool in the evaluation of the GCM hydrologic cycle and has helped quantify the influence of the more advanced land-surface model.

1. Introduction

Data assimilation systems have provided the climate and meteorology community with long-term atmospheric data sets that cover the globe and maintain consistency in time [*Bengsston and Shukla*, 1988; *Daley*, 1991]. The Goddard Earth Observing System (GEOS-1) data assimilation system produced one of the first long-term reanalyses to use a consistent modeling and assimilation system [*Schubert et al.*, 1993]. In this system, the prescribed land-surface wetness was computed from a bucket model forced with observations of monthly mean precipitation and near-surface atmospheric temperature [see, *Mintz and Serafini*, 1992; *Schemm et al.*, 1992; *Mintz and Walker*, 1993]. While the prescribed soil wetness has some advantages, the resulting GEOS-1 land-surface hydrologic budget was not balanced during the model integration.

Recently, the Off-line Land-surface GEOS Assimilation (OLGA) system has been developed to provide more detailed global surface data. OLGA is a global land-surface model driven by atmospheric data from the GEOS-1 reanalysis. The *Koster and Suarez* [1992, 1996] Mosaic land-surface model (LSM) provides the core of the surface physical parameterizations, including surface heat and water budgets.

This study evaluates the influence of OLGA's active land-surface calculations compared to observations and the GEOS-1 land-surface hydrology (which serves as a control). Runoff water is an important and sensitive component of surface hydrology. Here we define the source runoff water as the runoff water that is produced by a global model on the grid of the model. While runoff water observations are generally not available, the discharge of water at river mouths is routinely observed. Note the distinction between source runoff water and river discharge. Here we use a river routing model [*Miller et al.*, 1994] to determine simulated river discharge and compare with global observations.

To close the general circulation model (GCM) hydrology, the river routing model developed by *Miller et al.* [1994] moves GCM source runoff water through a river system to simulate the discharge of numerous basins around the Earth.

[1]Now at Raytheon, NASA Distributed Active Archive Center, Greenbelt, Maryland

Copyright 1999 by the American Geophysical Union.

Paper number 1999JD900346.
0148-0227/99/1999JD900346$09.00

The comparison of model and observed river discharge is a rigorous validation of a GCM surface model's ability to simulate important physical processes such as snowmelt. *Oki et al.* [1993, 1995] compare moisture flux convergence from the European Centre for Medium Range Weather Forecasting global operational analyses for up to 70 river basins. *Abdulla et al.* [1996] and *Nijssen et al.* [1997] have coupled a soil-vegetation-atmosphere transfer scheme with a parameterization of catchment scale processes to predict streamflow for a few river basins. *Oki and Sud* [1998] provide a detailed description of several recent GCM river routing models.

In the OLGA and GEOS-1 simulations, interaction between the surface soil water and the precipitation does not occur. While OLGA soil water is predicted in response to precipitation forcing, it does not change the precipitation. Soil water can influence precipitation processes in a variety of ways [*Mintz*, 1984; *Beljaars et al.*, 1996; *Bosilovich and Sun*, 1999], and ultimately, the interactions must be included in numerical simulations. An ongoing effort will couple the GEOS-1 data assimilation system with the Mosaic LSM. The interactive surface model has already been successfully implemented into the GEOS general circulation model. We will also present hydrology results from the coupled GEOS Mosaic LSM simulations.

2. Methodology

In this section, we summarize OLGA and GEOS-1 specifically focusing on the surface hydrology modeling strategies. The river routing model and the observations of precipitation and river discharge are also described.

2.1. Off-Line Land-Surface GEOS Assimilation (OLGA) System

The Off-line Land-surface GEOS Assimilation (OLGA) system [*Houser et al.*, 1998] is being developed as a test bed for developing land data assimilation strategies for the fully coupled GEOS data assimilation system. Therefore to the greatest extent that is reasonable the OLGA system has been designed to mimic the fully coupled system, with the vision of eventually implementing techniques developed off-line into the full GEOS data assimilation system. The OLGA system is proving to be an excellent resource for efficiently testing new land-surface data assimilation and modeling strategies and allows for the off-line replacement of often biased GCM land-surface forcing fields (such as precipitation and radiation) with observed quantities.

The OLGA system was implemented globally over land at a $2^\circ \times 2.5^\circ$ resolution for the 14 years of available GEOS-1 reanalysis forcing (1981 through 1995). The 3 hour GEOS-1 forcing data were linearly interpolated in time to the 5 min OLGA time step. The International Satellite Land-Surface Climatology Project initiative 1 land cover data specify vegetation in OLGA [*Meeson et al.*, 1995; *Sellers et al.*, 1995]. A 5 year OLGA simulation was used to spin up the inital state for the present simulation. The OLGA surface data sets are currently being offered as a supplement to the inactive land-surface present in the GEOS-1 reanalysis.

Mosaic LSM [*Koster and Suarez*, 1992, 1996] is the current land-surface model (LSM) implemented in OLGA. The Mosaic model is based on sound, well-accepted theory that has been proven by (1) its performance in several model intercomparison studies including the Project for the Intercomparison of Land Surface Schemes [*Henderson-Sellers et al.*, 1993]; (2) its ability to produce stable land-surface conditions and realistic climate simulations in the NASA Aries GCM [*Suarez et al.*, 1996]; and (3) the high correlation between Mosaic predictions and in-situ observations of surface fluxes and states made during several intensive field campaigns.

The Mosaic LSM was originally derived from the Simple Biosphere model developed by *Sellers et al.* [1986]. Mosaic, however, accounts for sub-grid-scale heterogeneity by dividing each GCM grid into homogeneous tiles. Furthermore, each tile is associated with a profile of model atmospheric grid points where turbulence is modeled. In OLGA, this permits partial surface atmosphere interactions but only near the surface, not with the large-scale environment.

The data that drive OLGA are the atmospheric state (temperature, moisture, and wind), the downwelling shortwave and longwave radiation, surface pressure, and precipitation. Mosaic maintains eight prognostic variables, which include the surface skin and deep soil temperatures, the canopy vapor pressure, and the water content of the snowpack, interception reservoir, and soil layers. A percentage of the incoming radiative energy to the land-surface is reflected, and the remainder that is absorbed is partitioned into upwelling longwave radiation, snowmelt, and sensible, latent, and ground heat fluxes. The partitioning of energy fluxes is controlled by a series of resistances that vary with environmental stress, and heat flow into the soil is performed using a force-restore method. Precipitation falling on the land-surface is partitioned into canopy interception, surface runoff, or infiltration into the first of three soil layers. Water diffuses between the layers, and can percolate out of the third layer. Water can be evaporated from the interception reservoir and the snowpack and can be extracted by plants from the top two soil layers for transpiration. *Koster and Suarez* [1996] discuss the water and energy conservation calculations in greater detail. For the present work, the calculation of runoff water is described below.

The rate of total source runoff R is generated in Mosaic as the sum of the surface runoff R_s and the baseflow or moisture diffusion flux out of the bottom of the lowest soil layer $Q_{3\infty}$:

$$R = R_s + Q_{3\infty} \tag{1}$$

The surface runoff rate, R_s is equal to the rate of rain throughfall P_T less infiltration:

$$R_s = P_T - \frac{W_1 - [W_1]_{\text{old}}}{\Delta t} \tag{2}$$

where W_1 is the moisture in the top layer, Δt is the time step length, and the subscript old denotes quantities calculated at the previous time step. The moisture in the top layer is updated by adding the smaller of either the throughfall onto

dry soil $P_{T-\mathrm{dry}}$ or the unused top layer moisture capacity $W_{1-\mathrm{add}}$:

$$W_1 = [W_1]_{\mathrm{old}} + \min(P_{T-\mathrm{dry}}, W_{1-\mathrm{add}}) \tag{3}$$

Mosaic soil hydrology calculations are divided into two sub areas, one that is fully saturated and the other whose degree of saturation is $W_{1-\mathrm{eq}}/W_{1-\mathrm{sat}}$. $W_{1-\mathrm{eq}}$ is the water content in the top soil layer that would be in equilibrium (according to Richards equation) with the water content in the middle soil layer, and $W_{1-\mathrm{sat}}$ is the moisture-holding capacity of the top soil layer. Given that W_1 is the total amount of water in the top soil layer, the saturated fraction f_{sat} can be computed as

$$f_{\mathrm{sat}} = \begin{cases} \frac{W_1 - W_{1-\mathrm{eq}}}{W_{1-\mathrm{sat}} - W_{1-\mathrm{eq}}} & W_1 > W_{1-\mathrm{eq}} \\ 0 & W_1 < W_{1-\mathrm{eq}} \end{cases} \tag{4}$$

Then, the throughfall mass falling on the dry fraction is

$$P_{T-\mathrm{dry}} = P_T(1 - f_{\mathrm{sat}})\Delta t \tag{5}$$

and the unused moisture capacity of the top layer is

$$W_{1-\mathrm{add}} = f(W_{1-\mathrm{sat}} - W_{1-\mathrm{eq}})(1 - f_{\mathrm{sat}}) \tag{6}$$

where f is the fractional coverage of precipitation.

Percolation out of the bottom of the lowest soil layer $Q_{3\infty}$ is computed with a bulk form of Richards equation in which only gravitational drainage operates, and the presence of bedrock is allowed to reduce the flow:

$$Q_{3\infty} = \rho_\omega K_3 \sin(\theta) \tag{7}$$

where θ is the bedrock angle, K_3 is the hydraulic conductivity of the lowest soil layer, and ρ_ω is the density of liquid water.

Mosaic LSM includes a bulk layer snow budget. The model predicts liquid water equivalent snow depending on new snowfall, sublimation, and snowmelt. When the snow melts, it is added to the canopy-intercepted water where the liquid water could evaporate, fall through to the soil, or refreeze [*Koster and Suarez*, 1996].

2.2. Goddard Earth Observing System (GEOS)

The GEOS-1 reanalysis has produced a multi-year global atmospheric data set for use in climate and weather studies [*Schubert et al.*, 1993]. The GEOS general circulation model is described by *Takacs et al.* [1994] and *Molod et al.* [1996]. *Pfaendtner et al.* [1995] document the data assimilation system. *Bosilovich and Schubert* [1998] discuss the GEOS-1 surface parameterization and interactions with the atmosphere.

A simple bucket model specifies the GEOS-1 monthly mean soil wetness off-line. The bucket model uses observed monthly mean precipitation and temperature as input [*Schemm et al.*, 1992], similar to the procedure of *Mintz and Serafini* [1992]. The prescribed soil wetness should provide lower boundary forcing that resembles observations and cannot drift toward unrealistic values. While modeled precipitation may be biased, the bias will not feed back into the atmospheric system through the soil wetness. However, without an interactive hydrologic balance at the surface, the long-term integration of evaporation no longer depends on the modeled precipitation. Runoff water is diagnosed from monthly mean soil water, precipitation, and evaporation after the completion of the model integration.

For each month during the period from January 1985 through December 1993, monthly mean runoff is computed by

$$R_o = P - E - \frac{\partial W}{\partial t}. \tag{8}$$

Here, P and E are the monthly mean precipitation and evaporation. R_o is the source runoff. The monthly mean change of soil water storage of water ($\partial W/\partial t$) is not small, and it cannot be neglected in the annual cycle. Because the storage of water is prescribed prior to the integration of the GEOS-1 reanalysis, this diagnostic computation can yield $R_o < 0$. Uncertainty of the evaporation based on the prescribed soil wetness and the inability of the storage of water to react to $P - E$ lead to negative values of runoff, which is unrealistic in the climate system [see also, *Arpe*, 1998]. *Oki et al.* [1993, 1995] used atmospheric moisture flux convergence data from a global operational analysis to compute approximate annual mean basin runoff. In some basins, they found moisture flux divergence ($R_o < 0$). To minimize this problem in the diagnosis of GEOS-1 runoff, we analyze each month separately. If at a grid point $R_o < 0$, then the value of runoff for that month is set to zero, and the negative value is integrated into a residual variable. The residual variable is saved to indicate the amount of imbalance in the GEOS surface hydrology. Hence, only positive values of runoff from equation 8 are included in the computation of GEOS-1 climatological annual cycle of runoff.

Presently, the Mosaic land-surface model (LSM) [*Koster and Suarez*, 1992, 1996] is being incorporated into the GEOS data assimilation system. The LSM is identical to that applied in OLGA. Hence future versions of the GEOS reanalysis will not be limited by the same deficiencies noted in this section. Some preliminary results of the GEOS general circulation model coupled with Mosaic LSM will also be presented.

2.3. River Routing Model

The river routing model was developed to provide closure to GCM hydrology budgets and to allow validation of GCM source runoff [*Miller et al.*, 1994]. Climate mean source runoff of GCMs (R_o) provides the forcing for the river routing (again, noting the difference between source runoff and river discharge defined earlier). To move the water from grid spaces to the river mouth, the routing model requires an algorithm for the river mass flow and a river direction file based on the topographic gradient. *Miller et al.* [1994] provide a complete list and map of all the river basins. Forty-seven river basins are defined in the river routing model with $2° \times 2.5°$ resolution.

Table 1. List of Experiments in This Study and Their Distinguishing Features and Differences.

Experiment Name	Details
GEOS-1	GEOS-1 9 years reanalysis data, limited surface model
OLGA	OLGA off-line Mosaic LSM 9 years simulation, driven by GEOS-1 reanalysis atmospheric forcing
GEOS Control	5 year GEOS GCM simulation, control run with limited surface model
GEOS-LSM	5 year GEOS GCM simulation, coupled with Mosaic LSM

The flux of water from a grid box (F in kg s^{-1}) is given by,

$$F = M \times \frac{u}{d}. \tag{9}$$

Where M is the river mass above the sill depth, d is the mean distance between the grid box and its downstream neighbor, and u is an effective flow velocity of water from a grid box to its downstream neighbor, depending on the downstream topography gradient. During a time step, the change in river mass in a grid box is given by,

$$M(t + \Delta t) - M(t) = S + \Delta t \Sigma F_{\text{IN}} - \Delta t F_{\text{OUT}}. \tag{10}$$

Where F_{OUT} is the flux of water that leaves a grid box, and ΣF_{IN} is the sum of all water entering a grid box. S is the source of water from grid space runoff. Eventually, the water is moved to the river mouth, where it is defined as the river discharge.

The resulting river discharge comparison with observations identifies strengths and weaknesses in the GCM hydrology, but it must be carefully examined. The river routing

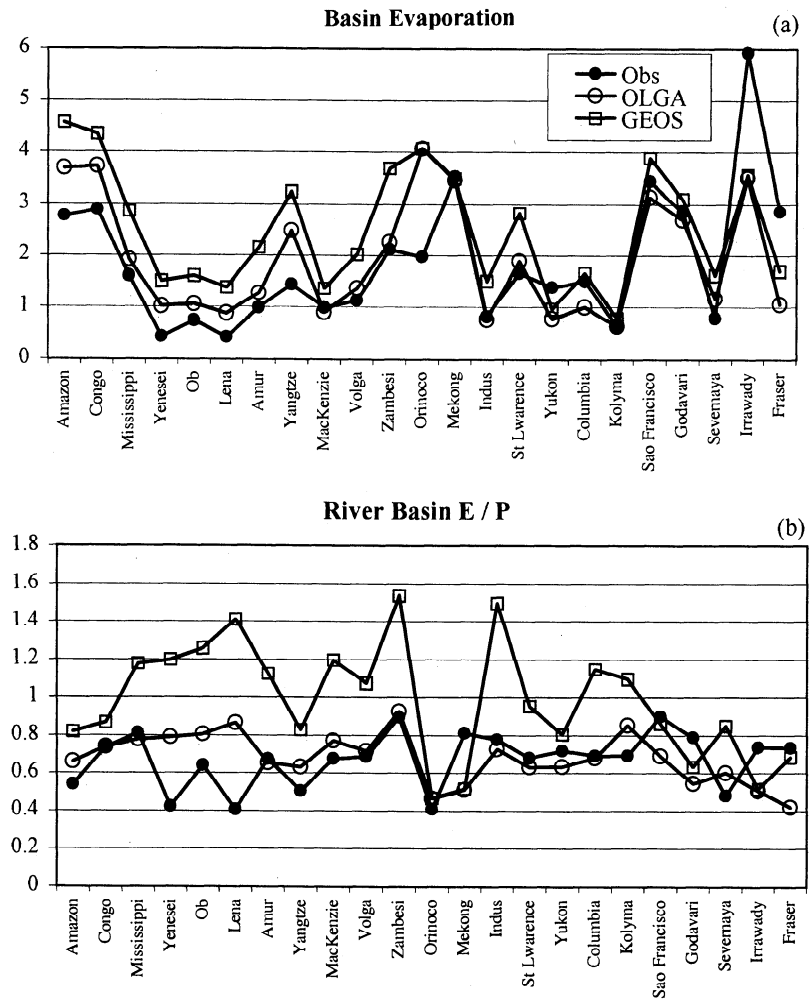

Figure 1. (a) Annual mean evaporation (mm d^{-1}) and (b) evaporation ratio (E/P). Sorted by decreasing basin area.

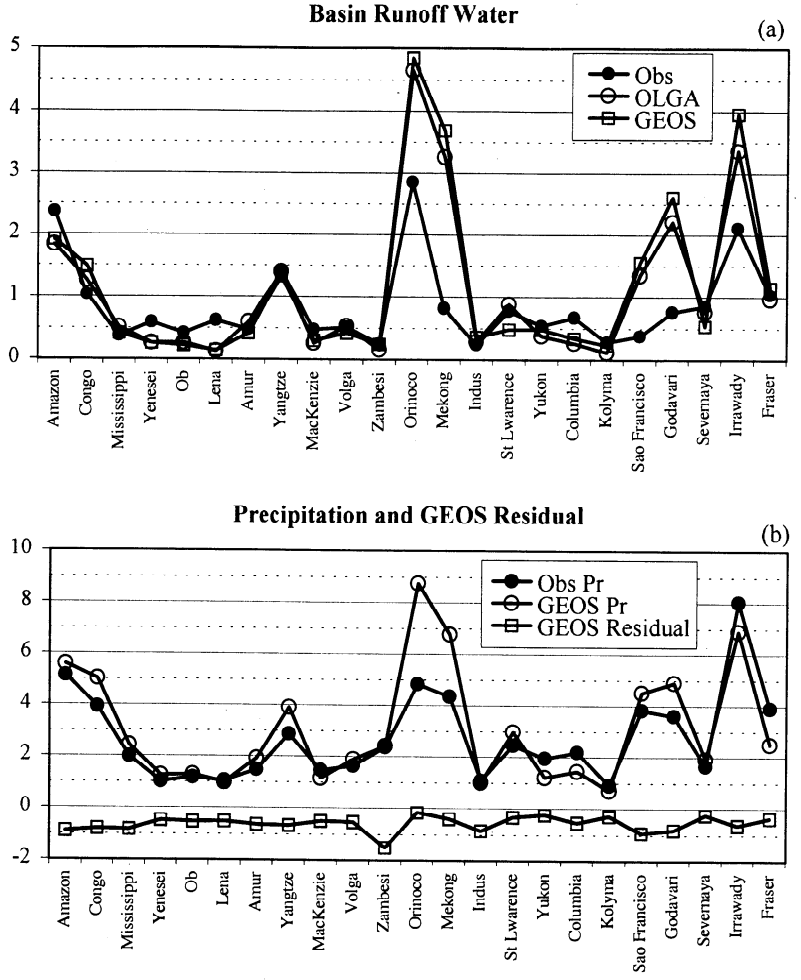

Figure 2. (a) Annual mean basin runoff water (mm d^{-1}) and (b) GEOS precipitation (which also forces OLGA), observed precipitation and the GEOS residual (mm d^{-1}).

model cannot ameliorate the effect of errors in GCM evaporation and precipitation on the river discharge, and may add error, due to incorrect specification of basin flow properties (topography, resolution, and flow velocity). Some processes are not included in the river routing model, such as freezing rivers (though the Mosaic LSM does freeze soil water) and ice flow.

2.4. Observations

We use two types of observed data for verification: river discharge from over 37 river basins and global gridded precipitation. The monthly mean river discharge data were provided by Global Runoff Data Center, Federal Institute of Hydrology, Germany [see also *Oki et al.*, 1993, 1995]. The observed monthly mean precipitation was merged Microwave Sounding Unit version-1 over oceans blended with rain gauge data over land at $4° \times 5°$ resolution. The climatological monthly mean values were computed for a 10 year period (1979-1988) [*Lau et al.*, 1996]. These precipitation data over land were also used to compute the GEOS-1 soil wetness boundary condition [*Schemm et al.*, 1992].

For comparison purposes, we approximate the basinwide observed evaporation using the climate mean river discharge and basin-averaged precipitation observations. For a climate average, the river discharge approximates area-averaged grid space runoff. Therefore by averaging equation (8) for the annual cycle, the climate mean basinwide evaporation can be computed by

$$E = P - R_d. \tag{11}$$

All the uncertainty in both precipitation and river discharge (R_d) will then be reflected in E.

3. Results

Table 1 summarizes the experiments used in this section. GEOS-1 identifies the original GEOS-1 data assimilation system experiment using a limited land-surface parameterization. OLGA identifies the off-line simulation of land-surface hydrology using the Mosaic LSM. To examine the interactive effects of the land-surface model on hydrology, we performed two GCM simulations (5 years duration). One simulation uses the same limited land-surface model as GEOS-1, and the other uses Mosaic LSM.

The comparison of GEOS-1 and OLGA will identify systematic differences between the land-surface processes in each model, given identical precipitation and atmospheric

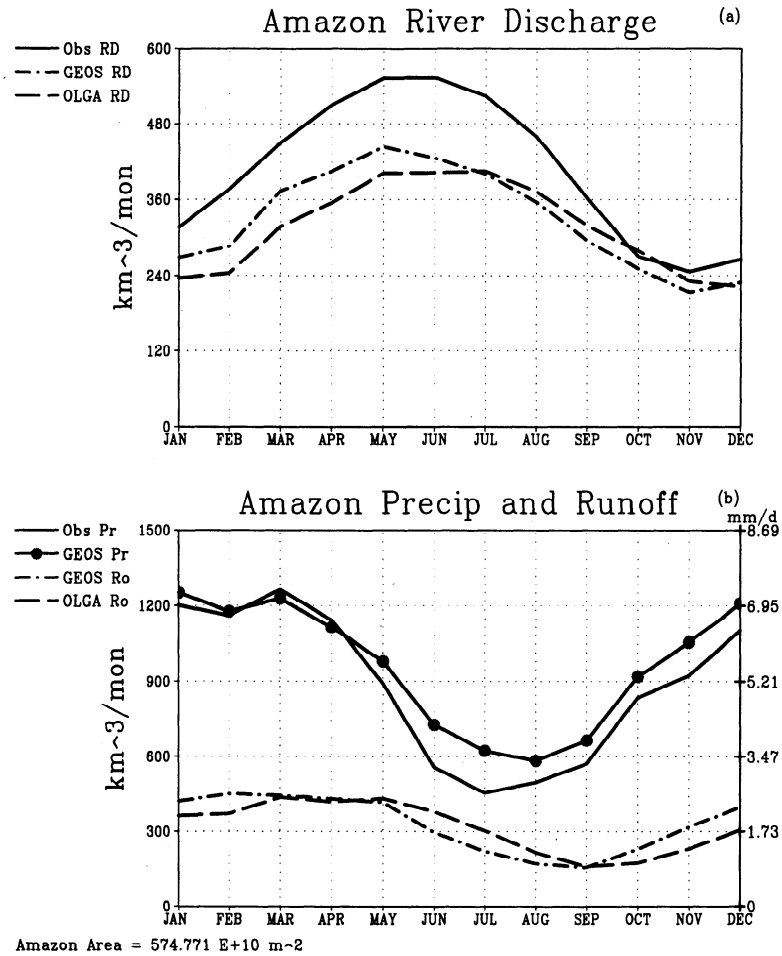

Figure 3. Annual cycle of (a) river discharge from the Amazon River basin for observations, OLGA, and GEOS-1, and (b) precipitation and model runoff.

forcing. This is an important first step in evaluating the land-surface physics. Eventually, the modeling system will evolve into interactive land-atmosphere processes, and the precipitation will be strongly affected leading to complicated differences in land-surface hydrology.

3.1. Basinwide Climate Hydrology

We approximate the annual mean basinwide observed evaporation assuming that it is equal to the difference of annual mean precipitation and river discharge. Figure 1 shows the climate mean evaporation and evaporation ratio (E/P) for 23 of the modeled river basins (sorted by decreasing basin area). In most of the basins, and especially the largest, GEOS-1 tends to overestimate the evaporation. While OLGA's evaporation tends to be less than (or equal to) that of GEOS-1, it is still larger than the observed residual evaporation in many basins.

The lack of surface hydrology balance in GEOS-1 is apparent in the basinwide climate mean evaporation ratio (Figure 1b). In many basins, GEOS-1 evaporation ratio is unrealistic for a climate mean ($E/P > 1$). OLGA's evaporation ratio tends to be closer to observations, and it is always less than 1 for a basinwide climate average. The reason for this drop in evaporation is because OLGA conserves water in the soil, and in GEOS-1, the soil water does not interact with the evaporation. The precipitation that is used in OLGA is slightly overestimated in many basins (Figure 2b), which may lead to more evaporation or more runoff.

Figure 2 shows the observed annual mean river discharge observations and model basinwide average grid point runoff. There are a few river basins where OLGA and GEOS clearly have difficulty to simulate the hydrology. However, there are more basins where the differences from observations are not very large. An interesting result of the runoff comparison shows that the annual mean of the GEOS-1 runoff is similar to that of OLGA. Two factors play a role in this similarity. First, the precipitation in each balance is the same. Secondly, both systems are constrained to a hydrologic balance. For GEOS-1, the residual of the hydrologic balance (section 2.2, Figure 2b) counteracts the most excessive evaporation biases in computing runoff. The major differences between the two cases are in the representation of the annual cycle.

3.2. OLGA and GEOS-1 Annual Cycles

While there may be many sources of uncertainty in the simulated river discharge, much may still be learned about

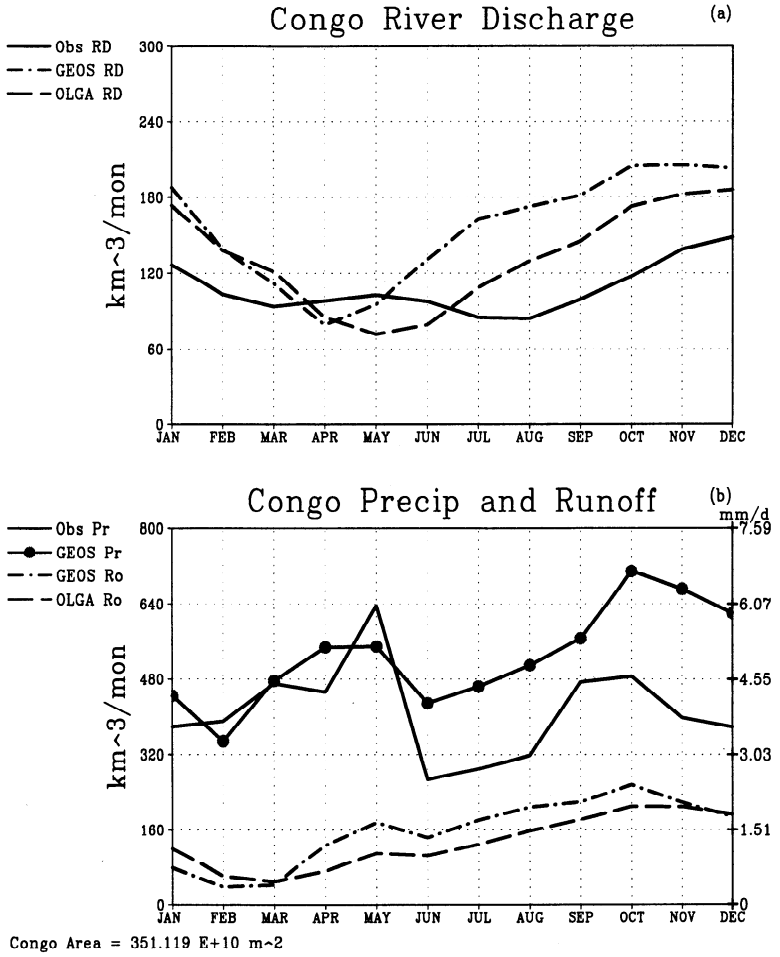

Figure 4. Annual cycle of (a) river discharge from the Congo River basin for observations, OLGA, and GEOS-1, and (b) precipitation and source runoff.

the model's hydrology. For example, river discharge from the Amazon is particularly difficult to simulate. *Lau et al.* [1996] find that many GCMs cannot generate as much river discharge as observed. Also, using the river routing model, coupled with the Goddard Institute for Space Studies GCM, *Miller et al.* [1994] strongly underestimate river discharge from the Amazon. In the present study, the Amazon precipitation is very large but comparable to observation (Figure 3). The source runoff for both OLGA and GEOS-1 are very similar, with OLGA slightly lagging behind GEOS-1. Overall, there are only small differences between the river discharge from the two models.

In the Congo river basin, GEOS-1 tends to overestimate precipitation ($\sim$ 1 mm d^{-1} annually), leading to the overestimate of river discharge in both OLGA and GEOS-1 (Figure 4). The phase of the OLGA river discharge annual cycle is lagged behind that of GEOS-1 and closer to the observations. The resulting improvement to the Congo river discharge is partially related to the physical soil processes in OLGA that slow the rate at which precipitation becomes runoff. While evaporation is improved in OLGA, the correction to the GEOS-1 runoff reduced the influence of the excessive evaporation on the runoff calculation (Figures 1a and 2a). However, there is improvement in the annual mean runoff from OLGA in the Congo which may be related to improved evaporation. Therefore in this region, the land-surface physics helped both the mean runoff and the annual cycle.

As discussed by *Boyle* [1998], GCMs tend to overestimate spring and summer rainfall amounts in the United States. This has been known for some time in the GEOS-1 data assimilation system [*Schubert et al.*, 1995], and it is quite apparent in this analysis (Figure 5). In the Mississippi River basin, the high summer precipitation dominates the simulate river discharge. *Beljaars et al.* [1996] show that increasing the surface evaporation causes increased precipitation. The poor summer precipitation in GEOS-1 could be related to the excessive evaporation from the simplistic surface representation. Likewise, if the new land-surface model can provide better surface evaporation in the Mississippi River basin, the precipitation may improve.

The northern river basins in OLGA exhibit substantial improvement of both source runoff and river discharge. The Volga River basin is a good example (Figure 6), but this result is also true for other basins (Amur, Ob, and somewhat noticeable in the Mississippi). The influence of the

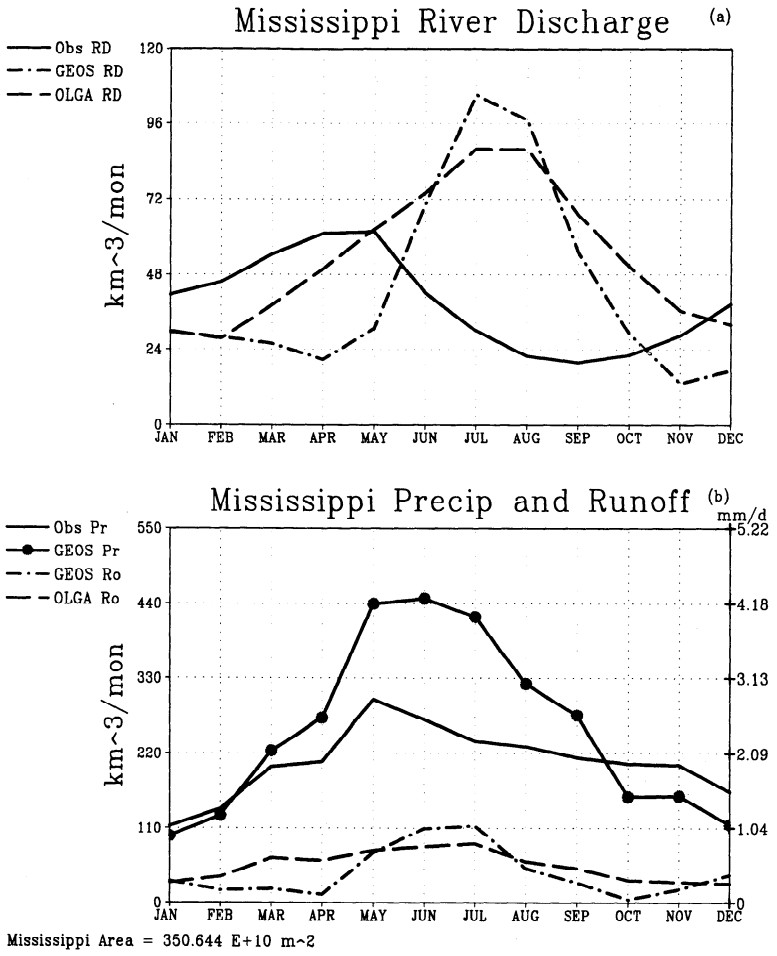

Figure 5. Annual cycle of (a) river discharge from the Mississippi River basin for observations, OLGA, and GEOS-1, and (b) precipitation and source runoff.

snowmelt in OLGA is quite apparent in the source runoff, especially compared to GEOS-1 (March and April source runoff in Figure 6b). Springtime snowmelt is not considered in the GEOS-1 land-surface model, which clearly affects the river discharge simulation. OLGA produces snowmelt runoff in the Volga River basin, but there is still a phase difference between OLGA and observations. This could be the result of either less winter precipitation (snow) or an underestimate of the river flow velocities in the river routing model.

The annual cycles show that for several basins, OLGA can produce improved river discharge compared with the GEOS-1. The improvements are related to the phase of the discharge. OLGA appears to slow down the rate at which precipitation becomes runoff (there is some residence time in the soil). This is especially noticeable in the northern river basins where snowmelt is important. However, not all basins show noticeable improvements. In section 3.3, we will generalize the river discharge error for a larger number of basins.

3.3. Error Analysis and Sensitivity

The river flow velocity (in equation 9) is computed as a function of the topographic gradient. In the vicinity of the river mouth, topographic gradients tend to be small. To prevent the flow velocity from becoming too small, a minimum flow velocity is imposed for all river basins (0.15 ms^{-1} is used in the experiments defined in Table 1). *Miller et al.* [1994] find that the river discharge is sensitive to this value. Because it appears that there may be lag in some of the simulated river discharge, we examine the influence of the minimum flow velocity on river discharge error.

River discharge errors for each simulation were computed for the river basins and global average following *Miller et al.* [1994 equations (10) and (12)]. The observed river discharge normalizes the error, so a value of zero indicates complete correspondence between model and observation. For individual basins, these values represent a combination of precipitation and evaporation errors, as well as the river routing. However, the normalized global runoff error is weighted by normalized monthly mean precipitation error. Figure 7 shows that in almost all of the river basins, OLGA river discharge error is either smaller than or the same as in GEOS-1. This holds for larger as well as smaller basins.

In the present models, global error from the Mosaic LSM (either OLGA or GCM-LSM simulation) is generally smaller compared to their control counterparts (Figure 8a). For reference, *Miller et al.* [1994] found a value of 0.566 global river discharge error in their simulations. In each set of

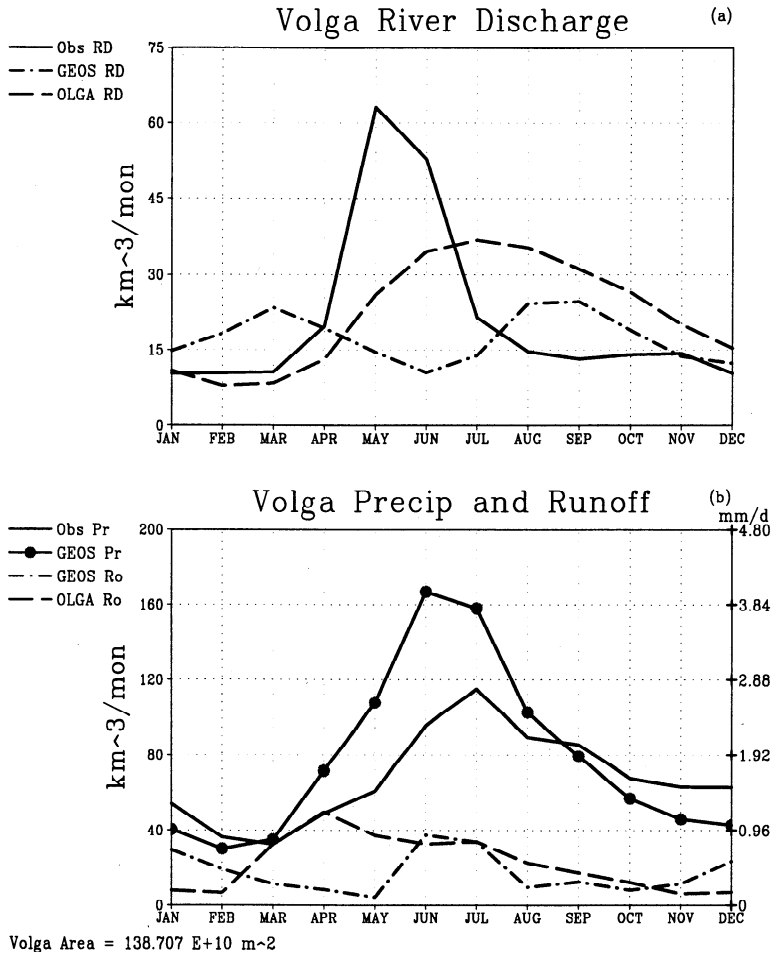

Figure 6. Annual cycle of (a) river discharge from the Volga River basin for observations, OLGA, and GEOS-1, and (b) precipitation and source runoff.

experiments, the simulation that includes the Mosaic LSM tends to reduce the minimum global error by approximately 0.05 (compared to the respective simulations with the simplified land-surface model). The OLGA river discharge improves for increasing minimum flow velocity (to 0.507 at 0.30 ms^{-1}), while the GEOS-1 lowest error occurs for smaller minimum flow velocities (0.570 at 0.15 ms^{-1}). This indicates that a process in OLGA is slowing down the movement of water from precipitation to the river discharge compared to GEOS-1. The storage, vertical diffusion, and baseflow of water in the more physical land-surface model will contribute this time lag.

The river discharge error for several river basins in the OLGA simulation is examined more closely (Figure 8b).

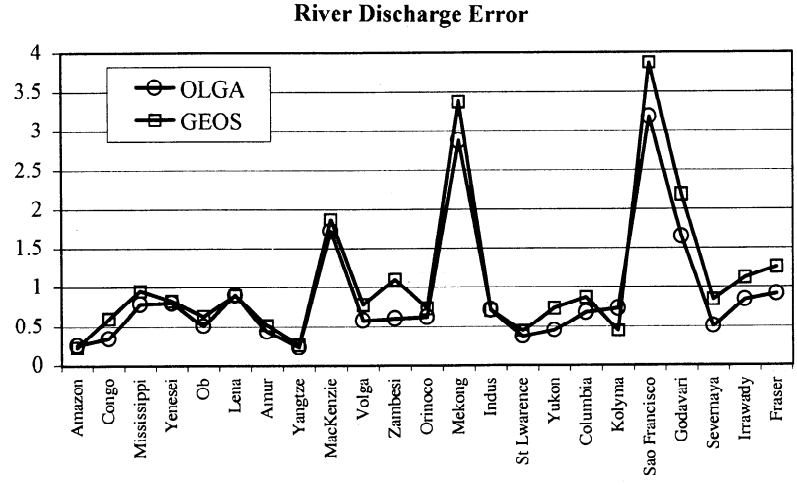

Figure 7. River discharge errors (following *Miller et al.* [1994]) for the GEOS-1 and OLGA experiments.

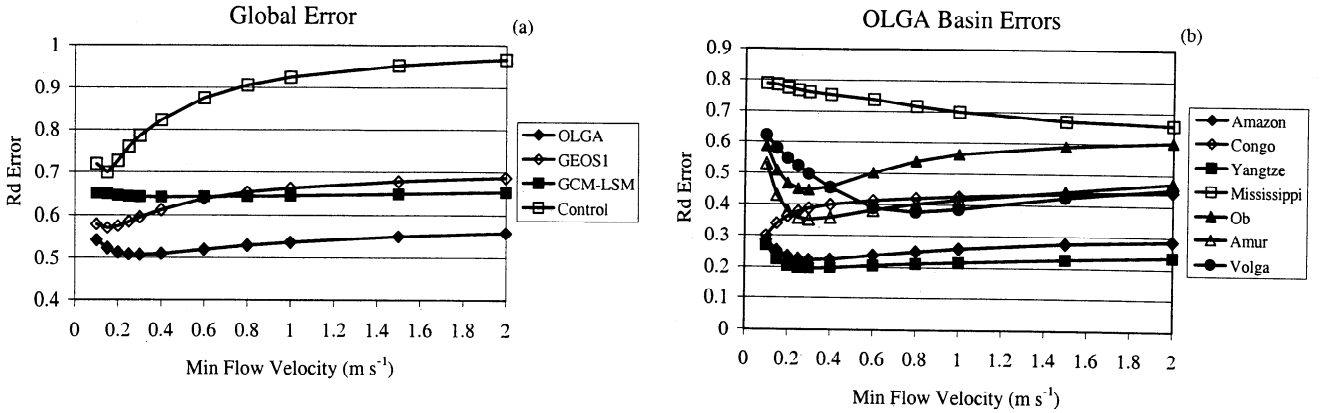

Figure 8. (a) Globally weighted river discharge error (using 37 basins) and (b) OLGA river discharge error of various river basins for different minimum flow velocities.

Four of the selected river basins (Amur, Ob, Amazon, and Yangtze) reflect the OLGA global error, with minimum error values occurring at 0.30 ms^{-1}. The Ob and Amur river discharge error decreases rapidly for small changes of low flow velocity. The Volga river error continues to decrease for fairly high values of the speed (0.80 - 1.0 ms^{-1}). This is related to increasing the speed at which the snowmelt water reaches the river mouth (see also Figure 6).

The difficulty in choosing a minimum flow velocity representative of all basins is apparent in the error for the Mississippi and Congo basins. The Mississippi error starts at a high value (probably related to the precipitation error in summer) and decreases with higher speeds. The Congo, however, has its lowest error with lower velocity, and the error increases with increasing speed. The simulated Congo river discharge annual cycle leads the observations and can-

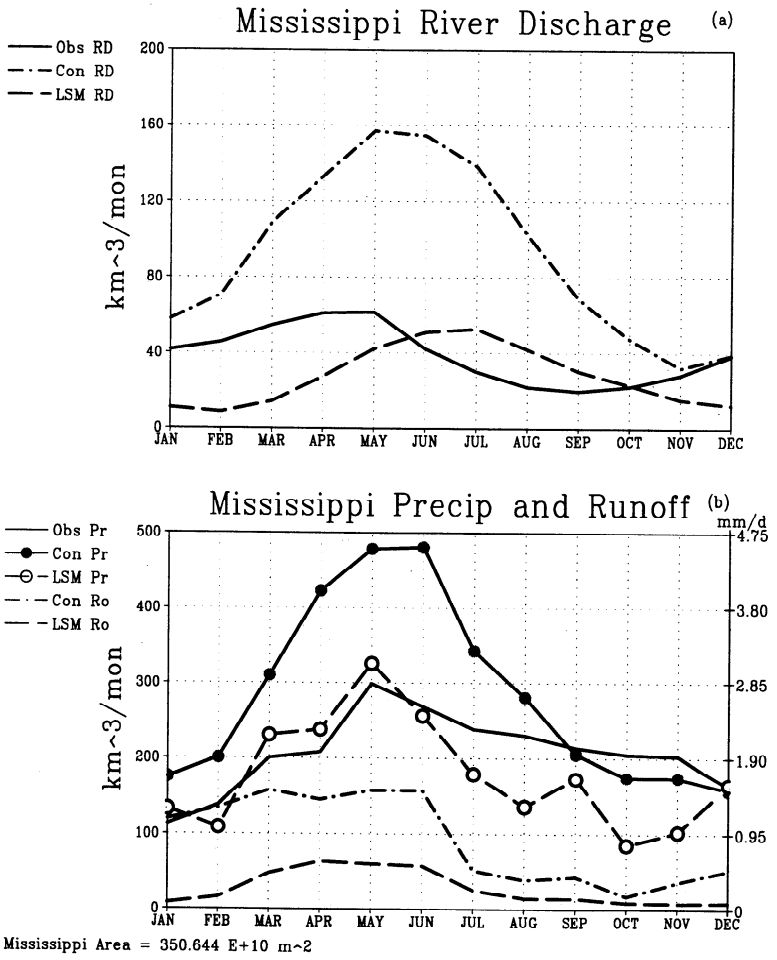

Figure 9. Annual cycle of (a) river discharge from the Mississippi River for observations, GCM-LSM, and the GCM control, and (b) precipitation and source runoff.

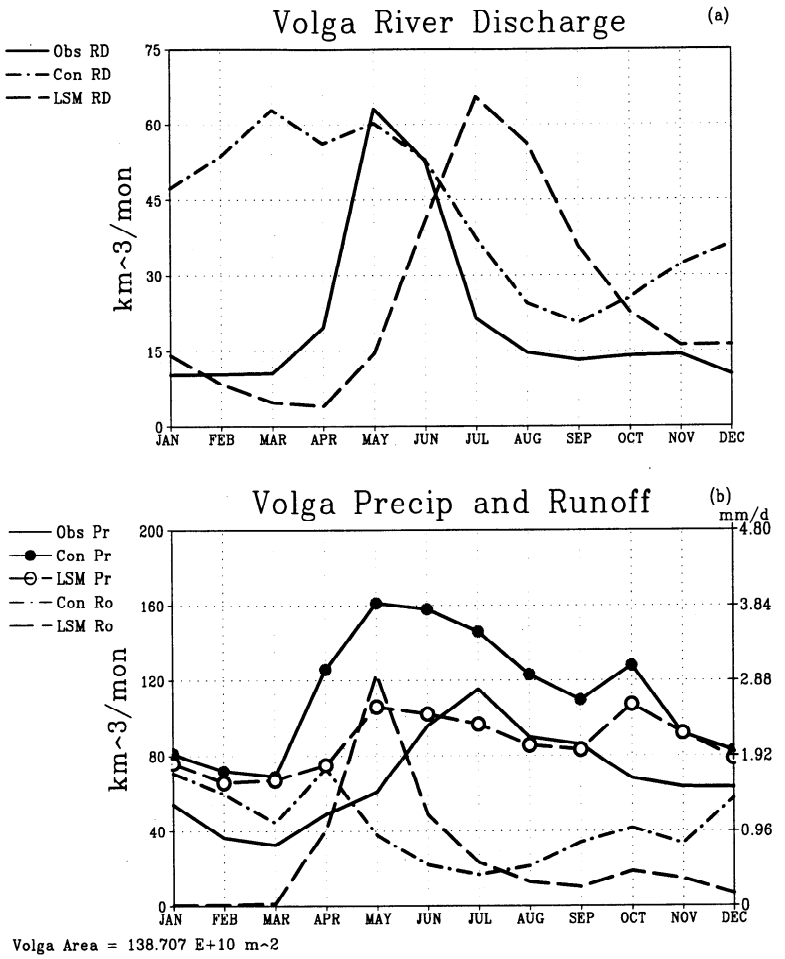

Figure 10. Annual cycle of (a) river discharge from the Volga River basin for observations, GCM-LSM, and the GCM control, and (b) precipitation and source runoff.

not benefit from increasing the minimum velocity (Figure 4). In future work, we will analyze whether the spatial error in precipitation influences the simulated discharge. We have not attempted to optimize the river routing simulations presented here because each GCM, as well as each river basin, requires improved or optimized values that describe the river flow.

3.4. GEOS GCM With Interactive Land-Surface Processes

In the previous discussion, the coupled land-surface interactions are not included in either the OLGA or the GEOS-1 systems. Soil wetness will influence the precipitation, evaporation and the river discharge. An ongoing effort to incorporate the Mosaic LSM into the GEOS general circulation model has produced some preliminary results. Here we present results from the GCM coupled with the Mosaic LSM (GCM-LSM) and a GCM "control" using the same surface parameterization as in GEOS-1 (Table 1). The GCM control runoff water was determined in the same way as GEOS-1. The GCM resolution is $4° \times 5°$, and both GCM cases were integrated for 5 years. Note that the GEOS-1 reanalyses include observational data assimilated into the GCM global system. In this experiment, the GCM simulations do not include the assimilated observations.

The influence of the coupled system on the Mississippi River basin precipitation is quite substantial (Figure 9). In the control simulation, the precipitation is very large in spring and summer, much like that of GEOS-1, leading to a substantial overestimate of the river discharge. With the coupled GCM-LSM, the spring and summer precipitation are much less than control and closer to observations. However, autumn precipitation, which is a valuable recharge source in the annual hydrologic cycle, is underestimated. This leads to low springtime river discharge. For the climate mean over the entire annual period, both precipitation and river discharge are much closer to observed than the control.

The GCM-LSM simulation of snowmelt processes is much better than the Control simulation. The control Volga River basin exhibits large river discharge in the winter due to the lack of simulated snow processes. The GCM-LSM, however, includes snow processes and produces a strong snowmelt signature in the model source runoff during late spring (Figure 10). The resulting simulated river discharge shows a similar pattern to the observations, but lags 2 months behind. There is some indication that for this simulation the

early spring temperatures were too cold to permit snowmelt (maintaining the snow cover until late spring).

The interaction between the land-surface and the atmosphere greatly complicates these comparisons. Future work will evaluate these processes in more detail. The present results, however, indicate that the coupled GCM-LSM can improve the simulation of river discharge similar to the off-line OLGA simulations (Figure 8a).

4. Summary and Conclusions

Land-surface hydrology has been examined for the Off-line Land-surface GEOS Assimilation (OLGA) system and Goddard Earth Observing System (GEOS-1) data assimilation system using a river routing model. OLGA's hydrology is evaluated against GEOS-1 (which serves as a control case) and observations using a global river routing model [*Miller et al.*, 1994]. The river routing model moves monthly mean climatologic source runoff through river networks to simulate the river discharge from global river basins, which can be compared to observed climatologic river discharge.

In general, the more detailed physical processes incorporated into the OLGA system produce a more reasonable river discharge than the GEOS-1 reanalysis. The soil processes in OLGA slow the generation of source runoff and reduce the error in the annual cycle of most of the basin's simulated river discharge. Snowmelt processes included in OLGA have a positive effect on the annual cycle of river discharge and source runoff. The phase of snowmelt runoff was lagged behind observations in some examples. Improved or optimized river flow characteristics could help the phase in the simulated river discharge. The river routing model, however, was not optimized because simulation is sensitive to both the choice of GCM as well as each individual river basin.

Simulations with a coupled GCM-LSM indicated that the land-surface model has a substantial effect on the entire hydrologic cycle in the GEOS GCM. In general, the Mosaic LSM provided improvements to the hydrology. The snowmelt, again, appears to be improved over the GEOS-1 land-surface. However, the phase of the simulated discharge was two months too late in the Volga River basin. Also, the bias of precipitation in the Mississippi River basin was much lower in the coupled system. This effort will continue with longer GCM simulations and data assimilations. The river routing model has provided a useful tool in the evaluation of the GCM hydrologic cycle and has helped quantify the influence of the more advanced land-surface model.

Acknowledgements. We would like to express our thanks to J. H. Kim for providing the merged precipitation data, GRDC for the river discharge data and G. L. Russell for providing the river routing model and data files. The reviewers of the original manuscript provided several insightful comments that contributed to the final version. Discussions with Andrea Molod, Sharon Nebuda, Siegfried Schubert, Robert Dickinson and Randal Koster greatly helped the development of these experiments.

References

Abdulla, F. A., D. P. Lettenmaier, E. F. Wood, and J. A. Smith, Application of a macroscale hydrologic model to estimate the water balance of the Arkansas-Red River basin, *J. Geophys. Res.*, 101, 7449-7459, 1996.

Arpe, K., Comparison of fresh water fluxes in the ECMWF, NCEP and GEOS-1 reanalyses, in *Proceedings of the First WCRP International Conference on Reanalyses, WMO TD-876, WCRP-104*, pp. 97-100, World Meteorol. Organ., Geneva, 1998.

Beljaars, A.C.M., P. Viterbo, M. Miller, and A. Betts, The anomalous rainfall over the United States during July 1993: Sensitivity to land surface parameterization and soil moisture anomalies, *Mon. Weather Rev., 124*, 362 - 383, 1996.

Bengtsson, L., and J. Shukla, Integration of space and in situ observations to study global climate change, *Bull. Am. Meteorol. Soc., 40*, 1130-1143, 1988.

Bosilovich, M. G., and S. D. Schubert, A comparison of GEOS assimilated data with FIFE observations, *NASA Tech. Memo. 104606*, vol. 14, 1998.

Bosilovich, M. G., and W.-Y. Sun, Numerical simulation of the 1993 Midwestern flood: Land-atmosphere interactions, *J. Clim., 12*, 1490-1505, 1999.

Boyle, J. S., Evaluation of the annual cycle of precipitation over the United States in GCMs: AMIP simulations, *J. Clim., 11*, 1041-1055, 1998.

Daley, R., *Atmospheric Data Analysis*, Cambridge Univ. Press, New York, 1991.

Henderson-Sellers, A., Z.-L. Yang, and R. E. Dickinson, The project for the intercomparison of land surface parameterization schemes (PILPS), *Bull. Am. Meteorol. Soc., 74*, 1335-1349, 1993.

Houser, P., R. Yang, J. Joiner, A. Da Silva, and S. Cohn, Land Surface GEOS assimilation strategy, Data Assimilation Office Note, Goddard Space Flight Cent., Greenbelt, Md, 1998.

Koster, R. D., and M. J. Suarez, Modeling the land surface boundary in climate models as a composite of independent vegetation stands, *J. Geophys. Res, 97*, 2697-2715, 1992.

Koster, R. D., and M. J. Suarez, Energy and water balance calculations in the Mosaic LSM, *NASA Tech. Memo. 104606*, vol. 9, 1996.

Lau, K.-M., J. H. Kim and Y. Sud, Intercomparison of hydrologic processes in AMIP GCMs, *Bull. Am. Meteorol. Soc., 77*, 2209 - 2227, 1996.

Meeson, B. W., F. E. Corprew, J. M. O. McManus, D. M. Myers, J. W. Clos, K.-J. Sun, D. J. Sunday, P. J. Sellers, *ISLSCP Initiative I, Global Data Sets for Land-Atmosphere Models, 1987-1988*, volumes 1-5, [CD-ROM], NASA, Greenbelt, Md., 1995.

Miller, J. R., G. L. Russell, and G. Caliri, Continental-scale river flow in climate models, *J. Clim., 7*, 914 - 928, 1994.

Mintz, Y., *Global Climate*, Cambridge Univ. Press, New York, 233 pp., 1984.

Mintz, Y., and Y. V. Serafini, A global monthly climatology of soil-moisture and water-balance, *Clim. Dynam., 8*, 13 - 27, 1992.

Mintz, Y., and G. K. Walker, Global fields of soil moisture and land surface evapotranspiration derived from observed precipitation and surface air temperature, *J. Appl. Meteorol., 32*, 1305 - 1334, 1993.

Molod, A., H. M. Helfand, and L. Takacs, The climatology of parameterized physical processes in the GEOS-1 GCM and their impact on the the GEOS-1 Data Assimilation System, *J. Clim., 9*, 764 - 785, 1996.

Nijssen, B., D. P. Lettenmaier, X. Liang, S. W. Wetzel and E. F. Wood, Streamflow simulation for continental-scale river basins, *Water. Resour. Res., 33*, 711 - 724, 1997.

Oki, T., and Y. C. Sud, Design of total runoff integrated pathways (TRIP): A global river channel network (on line), *Earth Inter., 2*, 1998. (Available at http://EarthInteractions.org)

Oki, T., K. Musiake, K. Masuda, and H. Matsuyama, Global runoff estimation by atmospheric water balance using ECMWF data set, in *Macroscale Modeling of the Hydrosphere*, edited by W.

B. Wilkinson, pp. 163 - 171, Int. Assoc. of Hydrol. Sci. Press, Oxfordshire, England, 1993.

Oki, T., K. Musiake, H. Matsuyama, and K. Masuda, Global atmospheric water balance and runoff from large river basins, in *Scale Issues in Hydrological Modeling*, edited by J. D. Kalma and M. Sivapalan, pp. 411 - 434, Advanstar Comm., Chichester, England, 1995.

Pfaendtner, J., S. Bloom, D. Lamich, M. Seablom, M. Sienkiewicz, J. Stobie, and A. da Silva, Documentation of the Goddard Earth Observing System Data Assimilation System - Version 1, *NASA Technical Memorandum No. 104606, vol. 4*, Goddard Space Flight Center, Greenbelt, MD, 1995.

Schemm, J., S. D. Schubert, J. Terry, and S. Bloom, Estimates of monthly mean soil moisture for 1979-1989, *NASA Technical Memorandum No. 104571*, Goddard Space Flight Center, Greenbelt, MD, 1992.

Schubert, S. D., J. Pfaendtner, and R. Rood, An assimilated data set for Earth science applications, *Bull. Am. Meteorol. Soc., 74*, 2331 - 2342, 1993.

Schubert, S. D., C.-K. Park, C.-Y. Wu, W. Higgins, Y. Kondratyeva, A. Molod, L. Takacs, M. Seablom, and R. Rood, A multiyear assimilation with the GEOS-1 System: Overview and results, *NASA Technical Memorandum No. 104606, vol. 6*, Goddard Space Flight Center, Greenbelt, MD, 1995.

Sellers, P. J., et al., *An overview of the ISLSCP Initiative I Global Data Sets: ISLSCP Initiative I - Global Data Sets for Land-Atmosphere Models 1987-1988*, volumes 1-5, [CD-ROM] NASA, Greenbelt, Md., 1995.

Sellers, P. J., Y. Mintz, and A. Dalcher, A simple biosphere model (SiB) for use within general circulation models, *J. Atmos. Sci., 43*, 505-531, 1986.

Suarez, M. J., and L. L. Takacs, Documentation of the Aries/GOES dynamical core version 2, *NASA Tech. Memo. 104606*, vol. 5, 1996.

Takacs, L. L., A. Molod and T. Wang, Documentation of the Goddard Earth Observing System General Circulation Model - Version 1, *NASA Tech. Memo. 104606*, vol. 1, 1994.

M. G. Bosilovich, Universities Space Research Association, Data Assimilation Office, NASA GSFC Code 910.3, Greenbelt, MD 20771. (email: mikeb@dao.sfc.nasa.gov)

Runhua Yang, Distributed Active Archive Center, NASA GSFC Code 902, Greenbelt, MD 20771.

Paul R. Houser, Hydrological Sciences Branch, NASA GSFC Code 974, Greenbelt, MD 20771.

(Received August 28, 1998; revised January 12, 1999; accepted May 14, 1999.)